Quim. Nova, Vol. 35, No. 7, 1325-1328, 2012

Artigo

Ce – PROMOTED CATALYST FROM HYDROTALCITES FOR CO_2 REFORMING OF METHANE: CALCINATION TEMPERATURE EFFECT

Carlos Enrique Daza
Departamento de Química, Facultad de Ciencias, Pontificia Universidad Javeriana, Calle 40 nº 5-50, Carrera 7 nº 43-82, Bogotá, D.C., Colombia
Sonia Moreno and Rafael Molina*
Departamento de Química, Facultad de Ciencias, Universidad Nacional de Colombia, Av. K. 30 45-03, Bogotá, D.C., Colombia

Recebido em 25/7/11; aceito em 11/2/12; publicado na web em 15/6/12

Ce-promoted Ni-catalysts from hydrotalcites were obtained. The effect of calcination temperature on the chemical and physical properties of the catalysts was studied. Several techniques were used to determine the chemical and physical characteristics of oxides. The apparent activation energies of reduction were determined. Catalytic experiments at 48 L $g^{-1}h^{-1}$ without pre-reduction in CO_2 reforming of methane were performed. The spinel-like phase in these oxides was only formed at 1000 °C. The reduction of Ni^{2+} in the oxides was clearly affected by the calcination temperature which was correlated with catalytic performance. The catalyst calcined at 700 °C showed the greatest activity.

Keywords: hydrotalcite; calcinations; syngas.

INTRODUCTION

Hydrotalcites have been widely reported as excellent precursors of catalysts for many reactions that operate at high temperatures due to the high thermal stability of the mixed oxides derived.[1-5] Also, because the properties of the hydrotalcites can easily be manipulated by different methods of synthesis and/or chemical compositions, it is possible to obtain highly efficient catalysts in terms of activity, selectivity and stability under long-term operation.[6-8] Reports describe that mixed oxides from hydrotalcites are precursors of metal (or bimetal) nanoparticles during the reduction process which is particularly significant in particle size-sensitive catalytic reactions.[9-12] CO_2 reforming of methane is one of the catalytic reactions in which the influence of particle size on the activity, and especially on the formation of coke is reported as the main cause of catalyst deactivation.[13-15]

Recently, CO_2 reforming of methane has gained considerable interest because of the global need for the generation of new energy sources to replace oil. From this catalytic reaction, syngas with a H_2/CO molar ratio close to 1 is obtained, suitable for the production of liquid fuels by Fischer-Tropsch synthesis. Furthermore, the reactants are the two most available and cheapest carbon sources related to the greenhouse effect. However, the thermodynamic tendency for coke formation in commercial catalysts have made this process little industrialized.[13-15]

We have reported the use of different types of hydrotalcites and natural clays as catalyst precursors for CO_2 reforming of methane.[16-22] Specifically, in our work with hydrotalcites we have focused on the study of hydrotalcites of Ce-containing Ni-Mg-Al obtained by coprecipitation,[19,22] reconstruction[17,18] and self-combustion methods.[21] The work led to highly active catalysts that are both selective and stable, with strong basic properties, low particle sizes and low coke formation.

We have also reported important findings about the nature of the Ce-promoter and the structural, surface morphology and chemistry of Ce-promoted hydrotalcites. Also, we studied in detail the effect of Ce-promoter, showing that loads of 3% wt. by reconstruction allowed obtention of a catalyst with better performance.[18]

*e-mail: ramolinag@unal.edu.co

However, some effects on the catalyst have not yet been described, leaving some hypotheses unanswered. More specifically, some authors have demonstrated the great influence of calcination temperature on catalytic performance of the materials.[23-25] It is clear from the literature that there is no common criterion for selecting calcination conditions (temperature, time and rates) for obtaining mixed oxides from hydrotalcites. For these reasons, we posed the question: what is the effect of calcination temperature on the chemical and physical properties of Ce-promoted mixed oxides from hydrotalcites? Does calcination temperature influence the formation of Ni^0 active species and correlation with catalytic performance?

The above questions are addressed in the present paper. The effect of calcination temperature on the structural (XRD, XPS), morphological (SEM), reductive (H_2.TPR), textural (N_2.adsorption) and chemical (XPS and CO_2.TPD) properties of Ce (3% wt)- promoted mixed oxides from hydrotalcites by reconstruction calcined under different temperature conditions was studied. Also, the apparent activation energies in the reduction of Ni^{2+} and catalytic tests in CO_2 reforming of methane without dilution gas and pre-reduction to establish correlations with the physical and chemical properties of the solids were reported.

EXPERIMENTAL

Synthesis of mixed oxides

Ce 3% wt-promoted Ni-Mg-Al catalyst was obtained by the method of reconstruction as reported elsewhere.[17,18] The precursor was calcined at 500 °C (16 h), 700 °C (12 h), 800 °C (10 h) and 1000 °C (8 h).

Characterization of mixed oxides

The chemical composition of the precursor was determined by inductively coupled-plasma spectroscopy (ICPS) using a TJA IRIS 1000 Radial ICP-AES device.

The temperature programmed reduction (H_2-TPR) profiles were taken on a Chembet 3000 Quantachrome device with a thermal

conductivity detector. A total of 100 mg of sample (<250 μm) was previously degasified at 400 °C for 1 h under an Ar flow. The materials were reduced at 10 °C min^{-1} employing 10% v/v H_2/Ar at 30 mL min^{-1}. Water was removed before the TCD using a cryogenic trap.

Apparent activation energies in Ni reduction were determined by the Kissinger's method cited by Jankovic *et al.*.[26] Several Temperature-Programmed Reduction profiles (TPR), varying the rates of temperature (β), were performed and maximum temperatures of reduction (T_{max}) determined. From a plot of $\ln(\beta/T^2_{max})$ versus $1/T_{max}$ and fitting to a straight line, the apparent activation energy *Ea* can be calculated from the intercept and slope, respectively, according to Equation 1:

$$ln\frac{\beta}{T^2} = ln\frac{AR}{Ea} - \frac{Ea}{RTmax} \quad (1)$$

The X-ray diffraction (XRD) profiles were taken on a Shimadzu LAB-X XRD 6000 device with a Cu anode, utilizing a rate of 0.02 ºθ s^{-1}. The Scherrer method was employed for determining the Ni^0 particle size.

BET areas, $V_{micropore}$ and $V_{mesopore}$ were determined by N_2-adsorption using a Micromeritics 2020 device.

CO_2 uptake measurements were performed by Temperature Programmed Desorption of CO_2 (CO_2-TPD) by 100 μL CO_2 pulses using a Chembet 3000 (Quantachrome) device. A total of 100 mg of catalyst was pre-treated in He at 500 °C for 1 h and cooled to room temperature before pulses adsorption.

The scanning electron microscopy (SEM) images were taken with a Fei-Quanta 200 device.

The X-ray photoelectron spectroscopy (XPS) spectra of the mixed oxides were carried out on a Physical electronics model 5600 spectrometer equipped with a hemispheric analyzer and a multi-channel detector. The polychromatic radiation of Al-Standard (350 W, 15.0 kV) was employed for the high resolution analysis. Binding energies were corrected using the C_{1S} signal in 284.5 eV as the internal standard.

Catalytic tests

Catalytic tests were performed as per previously reported methodology.[18,19] The catalysts were not previously reduced and reactants were injected from room temperature, increasing to 700 °C at 10 k min^{-1}. Flow of reactants used was CH_4/CO_2 1/1 v/v ratio without dilution gas (WHSV = 48 L $g^{-1}h^{-1}$). The reactants and products were monitored using a mass spectrometer (ThermoOnix) connected online.

RESULTS AND DISCUSSION

The chemical composition of the precursor determined by ICPS was 8.96 ± 0.16% wt. of Al, 1.48 ± 0.08% wt. of Ce, 15.72 ± 1.14% wt. of Mg and 19.72 ± 0.76% wt. of Ni.

The profiles of H_2-TPR of the mixed oxides are given in Figure 1S, supplementary material. The oxides showed only one peak of reduction at high temperature that corresponds to the reduction of Ni^{2+} to Ni^0 present in solid solutions which confers a high degree of chemical and thermal stability. We have reported that the form of the reduction profiles does not depend on the presence of Ce due to its preferential placement on the surface of the oxide aggregates.[17] However, a shift of 15 °C to lower temperatures observed in the Ce containing oxides may suggest that Ce facilitates the reduction of Ni. The reduction peaks when the oxide was calcined at 500 °C showed form asymmetry for lower temperatures which was not evident at the other calcination temperature. This result is probably related to the crystallinity of the oxides which clearly increases with increasing calcination temperature (Figure 2S, supplementary material). Hu[27] suggested two possible types of reducible species in solid solutions: NiO surrounded by MgO and NiO surrounded by NiO. The first type of NiO cannot be reduced because NiO is isolated (and diluted) by MgO while the reduction of the second type can take place because of lower interactions. Thus, this leads us to think that increased interactions by the increase in crystallinity may hamper reducibility of Ni^{2+}.

The oxide calcined at 1000 °C, meanwhile, had a reduction peak symmetrical at very high temperature for the reduction of Ni^{2+} in the spinel-like structure which is of greater stability and crystallinity compared with the periclase-like phase observed at lower calcination temperatures (Figure 2S, supplementary material). When the catalyst was calcined at different temperatures, the temperatures of maximum reduction were clearly increased with the calcination temperature, thus demonstrating an increase in NiO-bulk interactions.

XRD results showed that the spinel-like phase formation occurred only at 1000 °C. Some authors have reported the formation of this phase at temperatures lower than those found in the present study.[28-30] We believe that the formation of spinel-like phase both limits and decreases the reducibility of the catalyst which is directly related to the amount of active sites available for catalytic reaction.

In order to glean information to describe the process of reduction of these catalysts, the apparent activation energies were determined by Kissinger's method. As an example, Figure 3S, supplementary material, provides the method and results obtained in the case of the catalyst calcined at 500 °C. The reduction profiles (Figure 3S) showed an increase in the temperatures of maximum reduction (and in the area under the curve) when at greater heating rates. The changes in the form of the peak, especially for high β values, occur due to sizes of the small aggregates of the catalyst which generate heterogeneous packing in the reactor. Kinetics studies have reported an increased intensity peak with an increase in β because of an increase in dα/dt (α: reduced metal fraction) at higher heating rate, but despite this observation, no change or appearance of new peaks were observed.[31-33] The graphs of $ln(\beta/T_{max}{}^2)$ *vs.* $1/T_{max}$ (Figure 3S, supplementary material) were, for all calcination temperatures, straight lines, suggesting that in the range of β studied, the mechanism by which the reduction occurs was not modified.[26]

The apparent activation energies obtained are given in Table 1. The activation energy of the bulk NiO determined by the same method was 45 ± 5 kJ mol^{-1}, showing that the presence of Ni in the periclase and spinel-like lattice effectively causes an increase in the value of the energy of reduction due to the strong interactions that exist. The activation energies were higher with calcination temperature, showing that the different treatments of the catalysts not only cause changes in the temperatures at which reduction occurs but also in its kinetics. The values reported in this article are within the ranges found by other authors, and we attribute the disparities in data observed, in comparison with findings in the literature, to differences in methods of synthesis of the catalysts.[34] Despite the kinetic results of the reduction of the catalysts, the values of particle sizes (Table 1) showed no significant differences for each of the calcination temperatures, remaining in the range 9-12 ± 3 nm, less than or equal to sizes of other catalysts.[23,24]

These changes in reduction behavior can also depend on morphological changes as is shown in SEM images (Figure 4S, supplementary material). When the temperature was increased, superficial changes in the granules were evident, showing substantial superficial erosion and fracture of some large particles. In the same way, the drastic morphological change and increase in crystallinity of the material can be observed when calcined at 1000 °C, coherent with the results of the XRD. Particles size of 20-50 μm were observed when the solid was calcined below 700 ºC and of 30-100 μm at temperatures above 700 ºC. An increase in the Ni-bulk interaction due to sintering of crystals cannot be ruled out.

Table 1. Characterization for the oxides calcined at several temperatures

Catalyst	BET area ($m^2 g^{-1}$)	$V_{micropore}$ ($m^3 g^{-1}$)	$V_{mesopore}$ ($m^3 g^{-1}$)	Particle size (nm)*	CO_2 uptake (μmol m^{-2})**	E_a (kJ mol^{-1})
Calcined at 500 °C	78	0,00117	0,116	9 ±3	1,7 ±0,3	79 ±5
Calcined at 700 °C	58	0,00243	0,038	12 ±3	1,5 ±0,3	88 ±5
Calcined at 800 °C	42	0,00275	0,045	10 ±3	1,6 ±0,3	102 ±5
Calcined at 1000 °C	12	0,00104	0,045	10 ±3	1,5 ±0,3	125 ±5

*Determined by XRD after H_2-TPR runs. ** Determined by CO_2-TPD.

The BET areas and micro and mesopore volumes were modified with calcination temperature of catalysts (Table 1), evidencing a clear decrease, explained by the increase in crystallinity of the oxides and sintering of particle aggregates. A similar effect was observed in the total basicity of oxides, where a decrease in the values of CO_2-uptake per gram of catalyst was caused by the decrease in surface area of solids and apparent surface dehydroxylation at higher temperatures. However, despite declines, the basic values per m^2 remained unchanged for each of the catalysts (Table 1).

XPS was used to study the effects of calcination temperature on the formation of Ni and Ce species. In Figure 5S, supplementary material, the XPS spectra of the mixed oxides are registered. The $Ni_2p_{3/2}$ and $Ni_{2p1/2}$ electron spectra show main signals at 855.4 and 873.1 eV plus satellites at 861.4 and 879.4 eV, respectively (Figure 5S). The binding energies and separation of the *2p* doublet may correspond to NiO and/or $Ni(OH)_2$ and suggest that Ni is predominantly found as Ni^{2+}. The binding energies of the electron $Ni_{2p3/2}$ reported by different authors for NiO are between 854.2 and 854.6 eV; the shifts towards greater binding energies may result in the strong interactions produced by the formation of the solid solution.[35-37] The spectrum of the oxide calcined at 1000 °C exhibited shifts of +0.4 eV for the electron $Ni_2p_{3/2}$ and +0.3 eV for the level $Ni_{2p1/2}$, related with the formation of the spinel-like phase in which Ni has greater interactions in the crystalline structure. The CeO_2 spectrum was composed of different signals denominated *v, v", v"'* and *u, u", u"'* that describe the intensities of the photoelectrons $3d_{5/2}$ and $3d_{3/2}$. In the spectrum obtained (Figure 5S), the signals were observed at 898 eV (*v"*), 901 eV (*u*), 907 eV (*u"*) and 916 eV (*u"*). Comparison of the Ce_{3d} spectrum obtained in this work with those reported in the literature, confirmed that Ce is largely found as Ce^{4+} in mixed oxides. No shifts in Ce_{3d} signals were observed with calcination temperature.[38]

Figure 1 shows the results of the catalytic tests in CO_2 reforming of methane. As the reactants were injected at room temperature and the catalyst was not reduced in the first few hours of reaction, zero or very low activity was observed. Notably, the curves showed an "induction time" in which the catalyst is reduced before reaching high activity, the kinetics at this stage was different which is correlated with the activation energies obtained. The catalyst calcined at 500 °C was clearly reduced more rapidly and reached its maximum activity before the others.

The catalysts calcined at 500 and 700 °C had the highest activity of the series, with 700 °C proving the most active. On the other hand, the catalysts calcined at 800 and 1000 °C showed the lowest activity which is correlated with the limitation in the formation of active species of these catalysts due to high temperatures at which reduction occurs. This effect was much clearer in the case of the catalyst calcined at 1000 °C where the spinel-like phase formation significantly limited the reduction of Ni^{2+}.

H_2/CO molar ratios (Figure 1) showed that the catalysts have high selectivity, with values ranging from 0.8 to 1.0, that was practically independent of temperature at which they were calcined. Lower H_2/CO values were recorded during the first stage of the reaction, probably due to consumption of hydrogen in the *in situ* reduction of the catalyst.

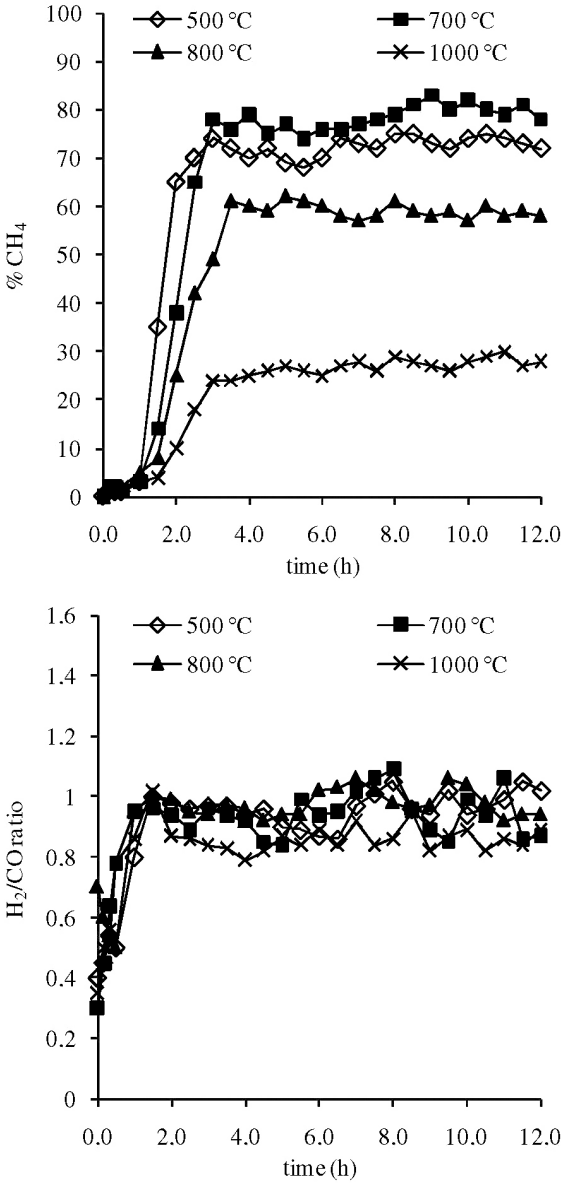

Figure 1. *CH_4 conversion and H_2/CO molar ratio in CO_2 reforming of methane at 700 °C for the oxides calcined at several temperatures*

CONCLUSION

The effect of the calcination temperature of Ni catalysts promoted with Ce derived from hydrotalcites was studied. It was established that the spinel-like phase only formed at 1000 °C and that the oxides

had strong basic properties and were Ni^0 nanoparticle precursors (9-12 nm). The kinetics of reduction of Ni^{2+} in the oxides is affected by the calcination temperature of the solid. The i*n situ* reduction of the catalyst is dependent on the calcination temperature, explaining the facts that catalysts calcined at 800 and 1000 °C had low catalytic activities in CO_2 reforming of methane. The catalyst calcined at 700 °C showed the highest activity.

SUPPLEMENTARY MATERIAL

Free access in PDF format available on-line at http://quimicanova.sbq.org.br.

ACKNOWLEDGEMENTS

The authors wish to specially thank Prof. F. Mondragon, at Quirema group, Universidad de Antioquia, Colombia, for his valuable support during C. Daza internship and Prof. C. R. Cabrera of Puerto Rico University for XPS measurements.

REFERENCES

1. Sychev, M.; Prihod'ko, R.; Erdmann, K.; Mangel, A.; van Santen, R. A.; *Appl. Clay Sci.* **2001**, *18*, 103.
2. Climent, M. J.; Corma, A.; Iborra, S.; Velty, A.; *J. Catal* **2004**, *221*, 474.
3. Kishore, D.; Kannan, S.; *J. Mol. Catal. A: Chem.* **2006**, *244*, 83.
4. Di Cosimo, J. I.; Díez, V. K.; Apesteguía, C. R.; *Appl. Clay Sci.* **1998**, *13*, 433.
5. Zhang, J.; Zhao, N.; Wei, W.; Sun, Y.; *Int. J. Hydrogen Energy* **2010**, *35*, 11776.
6. Climent, M. J.; Corma, A.; Iborra, S.; Epping, K.; Velty, A.; *J. Catal.* **2004**, *225*, 316.
7. Rao, M. M.; Reddy, B. R.; Jayalakshmi, M.; Jaya, V. S.; Sridhar, B.; *Mater. Res. Bull.* **2005**, *40*, 347.
8. Salmones, J.; Zeifert, B.; Garduño, M. H.; Contreras-Larios, J.; Acosta, D. R.; Serrano, A. R.; Garcia, L. A.; *Catal. Today* **2008**, *133-135*, 886.
9. Basile, F.; Fornasari, G.; Poluzzi, E.; Vaccari, A.; *Appl. Clay Sci.* **1998**, *13*, 329.
10. Nagaoka, K.; Jentys, A.; Lercher, J. A.; *J. Catal* **2005**, *229*, 185.
11. Olafsen, A.; Slagtern, Å.; Dahl, I. M.; Olsbye, U.; Schuurman, Y.; Mirodatos, C.; *J. Catal* **2005**, *229*, 163.
12. Takehira, K.; Shishido, T.; Shoro, D.; Murakami, K.; Honda, M.; Kawabata, T.; Takaki, K.; *Catal. Commun.* **2004**, *5*, 209.
13. Tao, X.; Bai, M.; Li, X.; Long, H.; Shang, S.; Yin, Y.; Dai, X. ; *Prog. Energy Comb. Sci.* **2011**, *37*, 113.
14. Ross, J. R. H. ; *Catal. Today* **2005**, *100*, 151.
15. Hu, Y. H.; Ruckenstein, E. In *Advances in Catalysis*; Bruce, C. G.; Knoezinger, H., eds.; Academic Press: Amsterdam, 2004, vol. 48, p. 297.
16. Daza, C.; Kiennemann, A.; Moreno, S.; Molina, R.; *Energy Fuels* **2009**, *23*, 3497.
17. Daza, C. E.; Cabrera, C. R.; Moreno, S.; Molina, R.; *Appl. Catal. A* **2010**, *378*, 125.
18. Daza, C. E.; Gallego, J.; Mondragón, F.; Moreno, S.; Molina, R.; *Fuel* **2010**, *89*, 592.
19. Daza, C. E.; Gallego, J.; Moreno, J. A.; Mondragón, F.; Moreno, S.; Molina, R.; *Catal. Today* **2008**, *133-135*, 357.
20. Daza, C. E.; Kiennemann, A.; Moreno, S.; Molina, R.; *Appl. Catal. A* **2009**, *364*, 65.
21. Daza, C. E.; Moreno, S.; Molina, R.; *Catal. Commun.* **2010**, *12*, 173.
22. Daza, C. E.; Moreno, S.; Molina, R.; *Int. J. Hydrogen Energy* **2011**, *36*, 3886.
23. Juan-Juan, J.; Román-Martínez, M. C.; Illán-Gómez, M. J.; *Appl. Catal. A* **2009**, *355*, 27.
24. Wang, H. Y.; Ruckenstein, E.; *Appl. Catal. A* **2001**, *209*, 207.
25. Zhang, S.; Wang, J.; Wang, X.; *J. Nat. Gas Chem.* **2008**, *17*, 179.
26. Jankovic, B.; Adnađevic, B.; Mentus, S.; *Chem. Eng. Sci.* **2008**, *63*, 567.
27. Hu, Y. H.; *Catal. Today* **2009**, *148*, 206.
28. Mokhtar, M.; Basahel, S. N.; Al-Angary, Y. O.; *J. Alloys Compd.* **2010**, *493*, 376.
29. Moroz, T.; Razvorotneva, L.; Grigorieva, T.; Mazurov, M.; Arkhipenko, D.; Prugov, V.; *Appl. Clay Sci.* **2001**, *18*, 29.
30. Pereira, H. B.; Polato, C. M. S.; Monteiro, J. L. F.; Henriques, C. A.; *Catal. Today* **2010**, *149*, 309.
31. Agula, B.; Ren, T.; Zhao, X.; Zhaorigetu, B.; Yuan, Z.; *J. Nat. Gas Chem.* **2011**, *20*, 232.
32. Heidebrecht, P.; Galvita, V.; Sundmacher, K.; *Chem. Eng. Sci.* **2008**, *63*, 4776.
33. Monti, D. A. M.; Baiker, A.; *J. Catal* **1983**, *83*, 323.
34. Fornasari, G.; Gazzano, M.; Matteuzzi, D.; Trifirò, F.; Vaccari, A.; *Appl. Clay Sci.* **1995**, *10*, 69.
35. Czekaj, I.; Loviat, F.; Raimondi, F.; Wambach, J.; Biollaz, S.; Wokaun, A.; *Appl. Catal. A* **2007**, *329*, 68.
36. Medina, F.; Salagre, P.; Sueiras, J. E.; Fierro, J. L. G.; *Appl. Catal. A* **1993**, *99*, 115.
37. Wrobel, G.; Sohier, M. P.; D'Huysser, A.; Bonnelle, J. P.; Marcq, J. P.; *Appl. Catal. A* **1993**, *101*, 73.
38. Kim, D. K.; Stöwe, K.; Müller, F.; Maier, W. F.; *J. Catal.* **2007**, *247*, 101.

Ce – PROMOTED CATALYST FROM HYDROTALCITES FOR CO_2 REFORMING OF METHANE: CALCINATION TEMPERATURE EFFECT

Carlos Enrique Daza
Departamento de Química, Facultad de Ciencias, Pontificia Universidad Javeriana, Calle 40 nº 5-50, Carrera 7 nº 43-82, Bogotá, D.C., Colombia
Sonia Moreno and Rafael Molina*
Departamento de Química, Facultad de Ciencias, Universidad Nacional de Colombia, Av. K. 30 45-03, Bogotá, D.C., Colombia

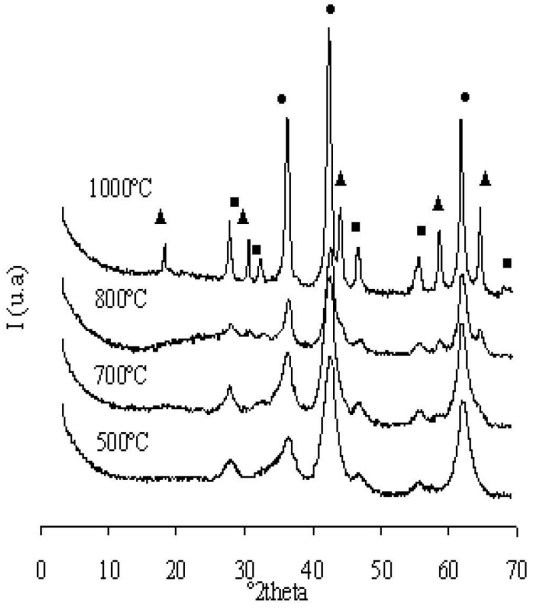

Figure 1S. *XRD for the oxides calcined at several temperatures. ▲ Spinel-like, ● Periclase-like, ■ CeO_2*

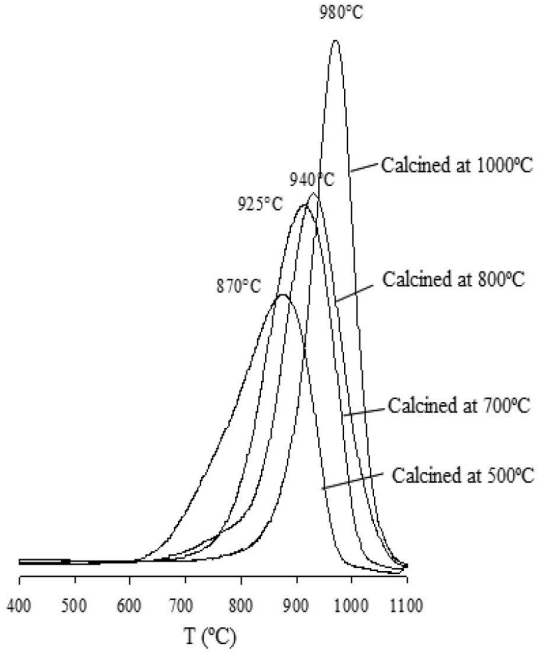

Figure 2S. *H_2-TPR for the oxides calcined at several temperatures*

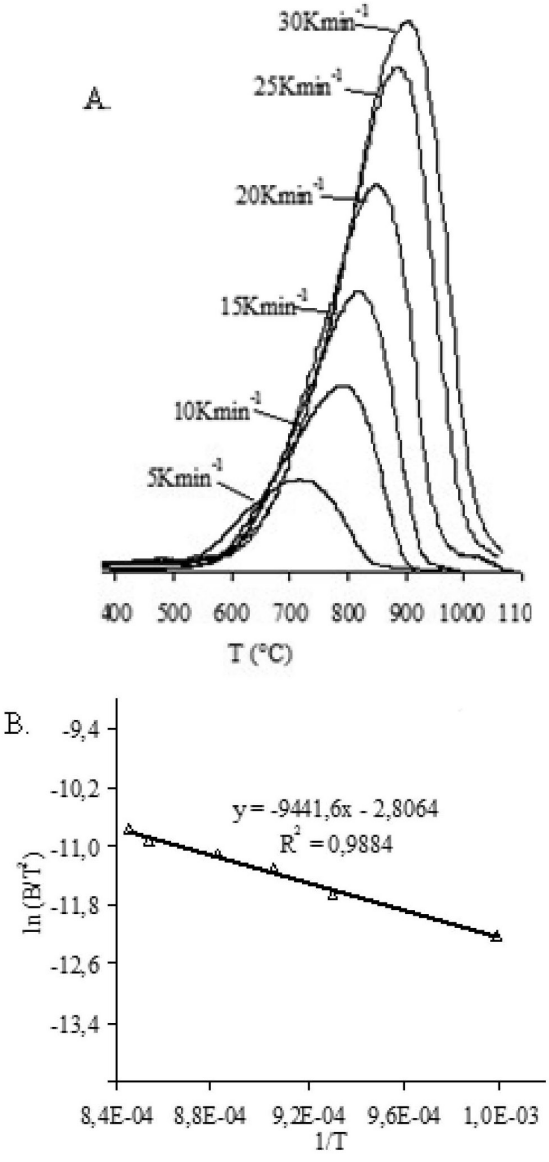

Figure 3S. *Determination of reduction activation energy for the catalyst calcined at 500 °C. A: Profiles at different rates of heating, B: Plot of $ln(\beta/T^2)$ vs. 1/T*

*e-mail: ramolinag@unal.edu.co

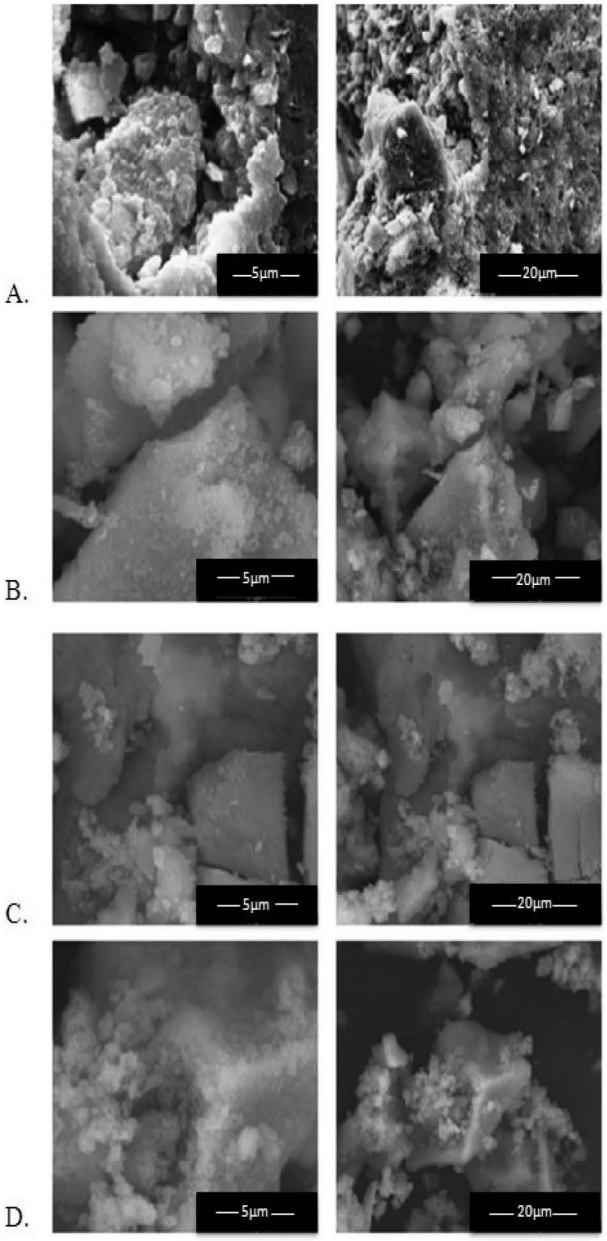

Figure 4S. *SEM for the oxides calcined at several temperatures, A) 500, B) 700, C) 800 and D) 1000 °C*

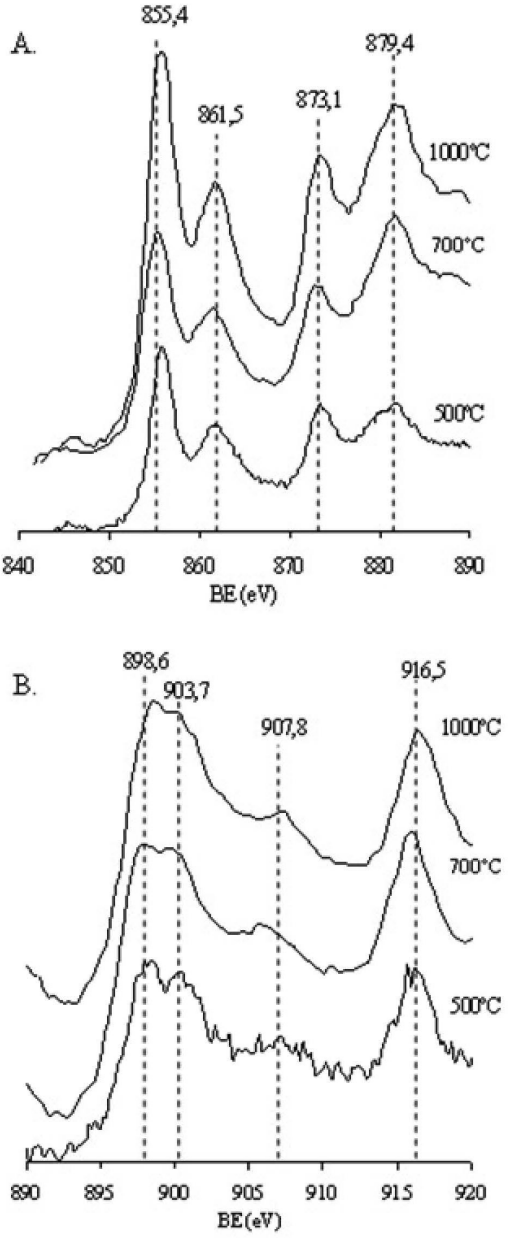

Figure 5S. *XPS spectra for the oxides calcined at different temperatures. A: Ni_{2p} zone. B: Ce_{3d} zone*